

# OPERATIONAL LIMITS AND LIMITING INSTABILITIES IN TOKAMAK MACHINES

H. R. Koslowski

Forschungszentrum Jülich GmbH, Institut für Plasmaphysik  
EURATOM Association, Trilateral Euregio Cluster,  
D-52425 Jülich, Germany

Keywords : Hugill diagram, Density limit, MARFE, Beta limit, Disruptions

## ABSTRACT

This article outlines the constraints for operation of tokamaks. The operating space is restricted by several limitations among which the plasma performance has to be optimized. Hard limits which lead ultimately to a disruption and may damage the first wall as well as soft limits resulting in a reduction of the energy content of the plasma can occur. The operational limits can be summarized in two general groups: excessive radiation from the plasma, and violation of global as well as local MHD stability boundaries.

## I. INTRODUCTION

The aim of fusion research is to achieve conditions for a magnetically confined burning plasma. The fusion power of a tokamak device scales like

$$P_{fus} \propto \beta^2 B^4 V, \quad (1)$$

where  $V$  is the plasma volume,  $B$  the toroidal magnetic field, and  $\beta$  the ratio between plasma pressure and magnetic field pressure. A high fusion power requires a large device and a high magnetic field. The machine size and the toroidal field strength are limited by technical and economical constraints. Maximizing  $\beta$  requires to raise the stored energy in the plasma and to enhance the plasma pressure in order to make best use of the externally applied toroidal field by appropriate means of tailoring the discharge.

There are only a few plasma parameters which can be controlled externally. The most important are the plasma density and the plasma current, which are both feedback controlled by acting on the gas fuelling rate and the induced loop voltage, respectively. The temperature, and hence the plasma pressure, can be increased by application of auxiliary heating by either injection of neutral beams or launching of electromagnetic waves in

the ion and electron cyclotron range of frequencies. The plasma itself can have different confinement states and a variety of regimes is reported in the literature. Most important (because it is foreseen to become the base operation mode in ITER) is nowadays the so-called H-mode (high confinement mode), observed in tokamaks with a poloidal divertor, where the stored energy in the plasma is increased due to an edge transport barrier [1]. Another scenario to optimize the plasma performance is the shaping of the current density distribution using appropriate means of non-inductive current drive and to establish the so-called optimized or reversed shear regime where internal transport barriers are created [2].

All of these scenarios are constraint by operational limits where in general two different kinds can be distinguished: (i) *soft limits* which lead to a degradation of the energy confinement, and (ii) *hard limits* where the plasma disrupts, i.e. the plasma current decays on a short time scale and the stored energy in the plasma is released to the wall.

The mechanisms leading to a deterioration of the confinement have to be studied carefully in order to avoid them, or to find means to stabilize these instabilities once they appear. Disruptions have to be prevented as far as possible because large forces act on the machine and the high energy flux hitting the first wall may cause very high erosion or even melting, and limits the lifetime of plasma facing components.

## II. THE HUGILL DIAGRAM

An overview on the achieved range of plasma parameters for a specific machine is usually given in the so called Hugill diagram. This diagram is a plot of the inverse safety factor at the edge,  $1/q_a$ , versus the Murakami number,  $\bar{n}_e R/B_t$ . In cylindrical geometry the edge safety factor is given by

$$q_a = 5a^2 B_t / (RI_p) \quad (2)$$

and from this it is obvious that the Hugill diagram is in principle a plot of the plasma current,  $I_p$ , versus the line averaged density,  $\bar{n}_e$ .

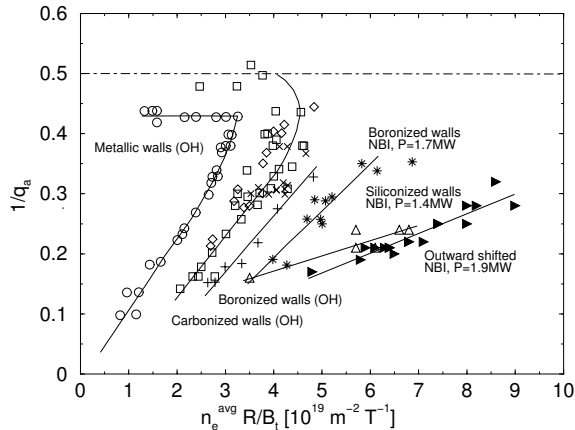


Figure 1: Hugill diagram for TEXTOR. (Figure from [3].)

Figure 1 shows the available operational space for the TEXTOR tokamak in Jülich, spanned by the data for various plasma conditions. Some of the operational boundaries can be seen in this graph. At first we notice the lack of points above  $1/q_a = 0.5$ . In this region the  $m = 2$ ,  $n = 1$  external kink mode is destabilized and leads to disruption of the discharge. This manifests a so called *hard boundary* which restricts the maximum plasma current for a given toroidal magnetic field (see eq. 2).

To the right of the graph we encounter the density limit, i.e. for a given plasma current there exists a maximum line averaged density. This boundary is empirically and the different groups of data points show that over the past years this limit has increased due to application of advanced wall conditioning methods [4]. Impurities released at the first wall can dilute the plasma and cause strong line radiation. When the total radiated power overcomes the heating power instabilities, normally leading to a disruption, are initiated. The application of low- $Z$  wall coatings helped to improve the situation and allowed to control the impurity content of the plasma. Strong additional heating permits higher radiation and pushes the density limit further.

A third limit, which is not very obvious, is near the left border of the graph. At very low densities electrons from the high energetic tail of the distribution function are continuously accelerated by the toroidal electric field and gain more energy per turn as they loose by collisions. The Maxwellian distribution is deformed and gets a non-thermal tail. This is called the runaway or slideaway regime. Operation at these plasma parameters has to be avoided because of high energetic electrons which may damage the first wall.

### III. RADIATION INSTABILITIES

A tokamak plasma has different sources for radiation: (i) bremsstrahlung due to electron-ion collisions, (ii) cyclotron radiation, (iii) line radiation from hydrogen/deuterium, impurities (N, O), and elements which are applied for wall coatings (Be, B, C, Si), radiation cooling (Ne), limiters (Mo, W), and diagnostic purposes (e.g. transport studies using short Ar puffs).

All these processes add up to the total power loss by radiation,  $P_{rad}$ , which has to be balanced by the heating power,  $P_{heat}$ . Under stationary conditions the heating power has to be larger than the radiated power, otherwise the plasma would cool down and give rise to the occurrence of instabilities.

The radiation from bremsstrahlung scales like

$$P_{br} \propto Z^2 n_e n_Z T_e^{1/2}, \quad (3)$$

where  $Z$  is the ion charge state,  $n_e$  and  $n_Z$  are the particle densities of electrons and ions, respectively, and  $T_e$  is the electron temperature. Under normal conditions this power can be easily supplied by the plasma heating systems.

The cyclotron radiation leads to a substantial radiation power density

$$P_c = e^4 / (3\pi\epsilon_0 m_e^3 c^3) B^2 n_e T_e, \quad (4)$$

where  $B$  is the magnetic field. Although this radiation power may become very large it is not of concern in fusion experiments. The reason is that the plasma is optically thick at the fundamental frequency and the emitted power is immediately re-absorbed. Loss of energy can occur at the harmonic frequencies where only a small fraction of this power is radiated.

The most important source for radiative power losses are the impurities. On the one hand they lead to an increase in bremsstrahlung (eq. 3), on the other hand they emit line radiation with a power density given by

$$P_R = L(T_e) n_e n_I, \quad (5)$$

where  $L(T_e)$  is called the radiation function for a specific impurity,  $n_I$  gives the impurity density in the plasma. The radiation functions are peaked at low temperatures and the radiation decreases towards higher temperatures. A general mechanism for the development of a radiation instability arises from this shape of the radiation function. A decrease in temperature due to excessive radiation will lead to an enhancement of the radiated power, which will cause a further drop in temperature and thus the process amplifies itself.

#### A. Density Limit

The Hugill diagram (figure 1) shows the density limit at the right edge. The region in the lower right

seems not to be accessible by the experiments. The density which can be achieved is higher when the plasma current is increased. Figure 1 indicates that the density limit depends on the wall coating and that an increase in the applied heating power helps to enhance the density limit. In the following we will briefly discuss two different reasons for the density limit. A much more detailed overview on the density limit observed in toroidal plasmas is given in a recent review article [5].

**A.1 Radiative collapse** When the electron density increases the electron temperature decreases. The line radiation from low-Z impurities is strongly enhanced. The plasma radiates mainly from the edge, where the impurity ions are not fully ionized. A poloidally symmetric radiation belt around the plasma develops. The density limit is reached when the radiated power equals the total heating power and the radiative collapse occurs. It is clear that either an increase in the auxiliary heating power or a decrease in the impurity content (due to low-Z wall coatings and glow discharge wall cleaning) can enhance the achievable density. The critical density scales as [6]

$$n_e^{crit} \propto (P_{heat}/(Z_{eff} - 1))^{1/2}. \quad (6)$$

The low effective charge state,  $Z_{eff}$ , as well as the large amount of heating power available in today's experiments would lead to very high values of the critical density. The onset of an asymmetric radiation instability, the so called MARFE will now determine the density limit.

**A.2 MARFE limit** The abbreviation MARFE means *multifaceted asymmetric radiation from the edge* [7]. This phenomenon is related to the transport of energy and recycling particles in the edge plasma. The MARFE is a zone of high radiation and occurs on the high field side (HFS) of the torus. A characteristic radiation pattern observed with a MARFE is shown in figure 2. The electron temperature in the MARFE is very low (a few eV) and the electron density becomes very high (several  $10^{20} \text{m}^{-3}$ ). The energy loss is mainly due to line radiation caused by ionization and charge exchange of incoming neutral particles. The onset conditions for the MARFE are strongly connected to the flux of recycling particles [8].

The density limit is found to be a general observation on all tokamaks and has been analyzed in detail by Greenwald [9]. He derived a very simple scaling law for the maximum line averaged density in a tokamak, namely

$$\bar{n}_{e,G} = \kappa \bar{j} \quad (7)$$

where  $\bar{j}$  is the averaged current density in the plasma and  $\kappa$  gives the elongation of the plasma cross section. This simple relation is called the *Greenwald limit* and

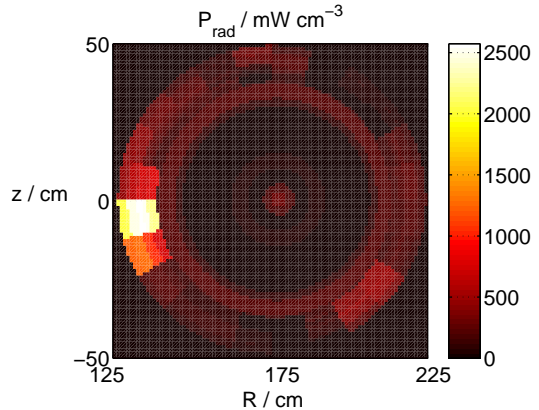


Figure 2: Tomographic reconstruction of the radiated power density during a MARFE in the TEXTOR tokamak. (Figure supplied by J. Rapp, EFDA-JET CSU Culham.)

gives a remarkably good estimate for the maximum density. It has been realized later that the Greenwald limit is connected to the onset of MARFEs.

The linear relation between density and plasma current is well seen in the Hugill diagram. The lines start with a linear slope before saturation due to the radiative collapse sets in.

Once the recycling of particles on the HFS of the torus has been identified to be the main cause for the limitation of density as long as sufficient heating power is available and the impurity content is low, the control of this flux might help to improve the limit. Small changes in the plasma position, i.e. a slight displacement of the plasma further to the low field side (LFS) can suppress the MARFE or delay the onset of this instability [10]. This finding has been utilized in recent work and by optimization of the plasma position electron densities as large as twice the Greenwald limit have been obtained [8]. A drawback of these experiments is, that the confinement quality of the plasma is degraded at these high densities. This finding is attributed to the strong gas puff needed to build up the density. Although high densities have been reached the performance of the discharge is not improved.

## B. Impurity Accumulation

Limiters made from a high-Z material like tungsten benefit from their high melting points and low sputtering rates. Nevertheless, a sudden onset of an instability caused by the transport properties of these high-Z impurities has been observed when the plasma conditions were unfavorable, i.e. above a critical density in ohmically heated discharges [11]. Atoms of the high-Z material are transported into the plasma center where they strongly radiate because they are only

partially ionized. The energy lost by radiation leads to a drop in the central electron temperature and a flattening of the temperature profile. As a consequence the temperature gradient decreases and the neoclassical inward flow velocity becomes larger which results in an increase of the concentration of high-Z atoms [12]. This enhances the radiation further until a hollow temperature profile develops and the plasma current is displaced. During the accumulation of the high-Z impurity the sawtooth oscillations (an MHD instability at the  $q = 1$  surface, a repetitive ramp-up of the central electron density and temperature followed by a sudden crash) are suppressed, because the current density in the center decreases and a  $q = 1$  surface is no longer present. As a consequence the electron density profile peaks, whereas the electron temperature profile becomes flat due to the enhanced radiated power from the center. The electrical conductivity of the plasma  $\sigma \propto f(Z_{eff}) T_e^{3/2}$  decreases, resulting in less current density in the center. This leads to a hollow profile of the safety factor  $q(r)$  [13]. Later during the accumulation process the safety factor on axis,  $q_0$ , reaches values larger than 2. The accumulation is followed by internal disruptions, which are a collapse of the central plasma parameters. This process can repeat several times. The internal disruption itself is due to the onset of MHD activity. The presence of double rational surfaces allows double tearing modes to occur (see chapter IV.G.).

#### IV. MHD STABILITY LIMITS

The magnetized plasma can be conveniently described within the magnetohydrodynamic model. The actual configuration of the toroidal plasma in the tokamak has to fulfill several constraints in order to be in an equilibrium (Shafranov equation, Mercier criterion). A variety of instabilities are derived from this description. The general procedure uses a linearization of the MHD equations and tests the reaction to a perturbation of the equilibrium, i.e. a displacement of the plasma. If this would lower the potential energy, the state of the plasma is unstable with respect to this mode.

The destabilizing forces originate either from the plasma current distribution or from the plasma pressure. The MHD modes are categorized into *ideal modes* (conservation of magnetic flux) which would even occur in a perfectly conducting plasma, and *resistive modes* (magnetic flux not conserved) which need a finite resistivity to be destabilized [14].

These modes can have different influence on the plasma, ranging from a deterioration of the confinement properties up to a termination of the discharge by a disruption. In general, the action of a mode on the plasma depends on the size upon which it grows and

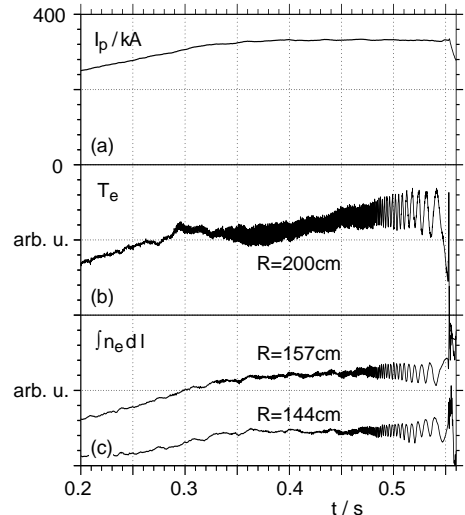


Figure 3: Onset of a  $m/n = 2/1$  tearing mode in TEXTOR followed by a disruption. The signals are: (a) plasma current, (b) electron temperature on the low field side close to the  $q = 2$  surface, (c) two channels of the HCN-interferometer on the high field side measuring on both sides with respect to the mode location. Note that the phase of the modulation is opposite on both signals, indicative for an island type mode.

on the transport of energy and particles associated with the mode (non-linear behaviour).

##### A. $q_a$ -Limit

The  $q_a$ -limit has already been mentioned when we discussed the Hugill diagram. The accessible range is restricted to the area  $1/q_a < 0.5$ , or  $q_a > 2$ , i.e. the safety factor at the edge cannot be smaller than 2. This gives an upper boundary for the plasma current dependent on the toroidal magnetic field (see eq. 2). When the  $q = 2$  surface lies outside of the plasma the  $m = 2$ ,  $n = 1$  external kink mode occurs. This is an ideal mode which is destabilized by currents flowing at the plasma surface. In the startup phase of discharges the ramp-up of the plasma current can trigger these surface kink modes (with  $m = \dots, 6, 5, 4, 3$ ) when  $q_a$  decreases and goes through these rational values, what is frequently seen on the signals from magnetic pick-up coils. When  $q_a$  decreases further these modes are stabilized again. A highly conducting wall closely surrounding the plasma surface can stabilize this mode, but in most present tokamaks the first wall is far away from the plasma in order to reduce the plasma-wall interaction. This is an example of a hard limit, i.e. when it is violated, the plasma will unavoidably disrupt.

##### B. Tearing Modes

Tearing modes are resistive instabilities driven by

current gradients in the plasma. The reconnection of magnetic flux and the development of magnetic islands is associated with these modes. The growth of tearing modes depends on the tearing parameter  $\Delta'$ , defined as

$$\Delta'(w) = \frac{1}{B_r} \left. \frac{\partial B_r}{\partial r} \right|_{r_s-w/2}^{r_s+w/2} \quad (8)$$

where  $w$  is the island width and  $r_s$  the radius of the rational surface of the mode. An approximation for the growth rate of these modes is given by

$$\frac{dw}{dt} \simeq \frac{\eta}{2\mu_0} \Delta'(w). \quad (9)$$

where  $\eta$  is the resistivity of the plasma. If  $\Delta' > 0$  the mode is destabilized and will grow until it reaches its saturated island size. An example of the onset of a  $m = 2, n = 1$  tearing mode, which is usually the strongest of these instabilities, is shown in figure 3. This mode can grow up to rather large island sizes. The transport across the island region is enhanced due to a short circuit of magnetic field lines between the inner and outer island boundaries. This mode can even initiate disruptions (as can be seen in figure 3 after  $t = 0.55$  s) due to the modification of the plasma current profile at the edge.

### C. The Ideal $\beta$ -Limit

For a high performance of the tokamak the ratio  $\beta_t$  between the plasma pressure and the magnetic field pressure,

$$\beta_t = 2\mu_0 \langle p \rangle / B_t^2, \quad (10)$$

has to be large in order to make best use of the externally applied toroidal field. ( $\langle p \rangle$  is the volume averaged plasma pressure.) The maximum plasma pressure which can be confined by a given magnetic field has been calculated by Troyon [15], taking into account ideal MHD instabilities as well as ballooning modes and the Mercier criterion. The calculations were performed for optimized profiles of the plasma current and the plasma pressure. It has been found that the  $n = 1$  free-boundary kink modes impose an upper limit on  $\beta$ . For the poloidal beta,  $\beta_p$ , where  $B_t$  in equation 10 is replaced by the poloidal field,  $B_p(a)$ , and for circular plasma cross section the scaling

$$\beta_p^{max} = 0.14 (R/a) q_a \quad (11)$$

was derived.

### D. Neo-Classical Tearing Modes

It is a common observation on many tokamak experiments that the ideal beta limit is only reached transiently, but stationary discharges are limited to a lower

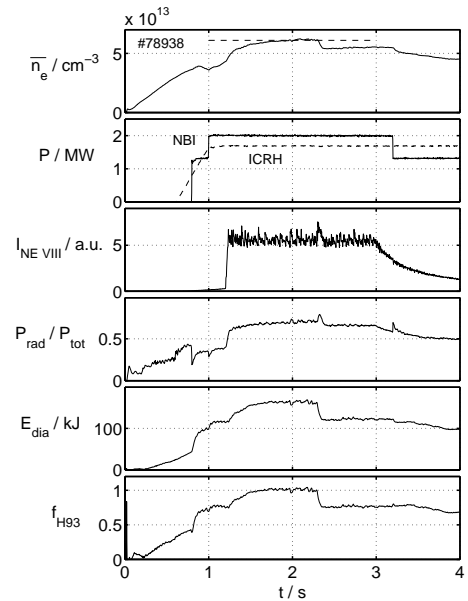


Figure 4: Confinement deterioration in a discharge with Ne seeding due to onset of a neo-classical 3/2 mode. The curves from top to bottom are: the line averaged electron density, the auxiliary heating power, the intensity of a Ne-VIII line (used for radiation feedback), the radiated power fraction, the stored energy, and the confinement quality factor with respect to ELM-free H-mode scaling.

value [16]. This behavior is found to be due to the onset of so called neo-classical tearing modes (NTM). An example for a discharge where the confinement degrades due to onset of a NTM is shown in figure 4 [17].

The growth of neo-classical tearing modes is described by the generalized Rutherford equation [16]. In addition to the tearing parameter  $\Delta'$  two different pressure driven contributions are included. One term is destabilizing and results from the loss of bootstrap current in the island, caused by the flattening of the pressure profile. The second term is stabilizing and originates from the polarization current within the island. The most important features of neo-classical tearing modes are: (i) The modes grow although the tearing parameter  $\Delta'$  is negative, and (ii) the growth of the mode requires a minimum island size, the so-called *seed island* which needs to be created by a MHD perturbation, e.g. a sawtooth crash in the core. A more detailed derivation of neo-classical tearing modes will be given elsewhere in this proceedings [18].

Neoclassical tearing modes have nowadays been recognized as a serious limitation of the energy confinement on nearly all tokamaks. The scaling of NTM onset with the plasma parameters predicts a low threshold for ITER and various mechanisms for active stabiliza-

tion have been applied or proposed: (i) Replacement of the loss in bootstrap current by electron cyclotron current drive [19], (ii) reduction of  $\Delta'$  by shaping of the plasma current distribution using lower hybrid current drive [20], and (iii) stabilization of the NTM by an externally applied static helical field [21]. By selecting a suitable beta it is even possible to obtain acceptable confinement in spite of a NTM [22].

#### E. Locked Modes

A locked mode is an MHD perturbation which does not rotate with the plasma fluid. Normally a growing MHD mode in the plasma slows down in rotation speed because of friction due to eddy currents in the wall and finally it locks, i.e. the rotation stops due to error fields which are created by slight misalignments of the external coils of the tokamak. The slowing down of a tearing mode and finally the locking to the wall is found to be a precursor to disruptions. It is experimentally found that these disruptions can be prevented when the mode is kept rotating using momentum input by tangential neutral beam injection [23].

#### F. Resistive Wall Modes

The ideal beta limit is determined by the external kink mode becoming unstable. This is often the limiting factor in advanced tokamak scenarios with a high bootstrap current fraction and broad current profiles. This mode can be stabilized when the plasma is surrounded by an perfectly conducting wall within a critical distance. A conducting wall with a finite resistivity will reduce the growth rate of the external kink to the inverse of the resistive time constant of the wall, making it therefore much smaller. This is called the *resistive wall mode* (RWM). Two possibilities for stabilizing RWMs are proposed: (i) dissipation of the free energy of the mode by plasma rotation, and (ii) an active feedback scheme which applies a field opposite to the RWM [24].

#### G. Double Tearing Modes

In ohmic tokamak discharges the profile of the safety factor adjusts itself according to the resistivity in the plasma. Under normal conditions, i.e. without accumulation of impurities the  $q$ -profile is monotonous, having the minimum on the magnetic axis and increasing towards the edge of the plasma. The magnetic shear

$$s = \frac{r}{q} \frac{dq}{dr} \quad (12)$$

is positive throughout the plasma. There are several situations when the shear becomes negative: (i) during the current ramp phase, (ii) when the conductivity in the center is decreased due to impurity accumulation,

or (iii) when a substantial amount of non-inductive current is driven off-axis. The latter case is often experimentally observed because transport barriers may build up in the vicinity of the minima in the safety factor profiles. These reversed shear  $q$ -profiles can have double rational surfaces like  $q = 1, 3/2, 2, 3, \dots$  giving rise to double tearing modes, i.e. coupled modes at the inner and outer rational surface, respectively. These modes destroy the confinement between double rational surfaces and can result in violent collapse events in the plasma, especially when more than one double rational surface is present and mode coupling can influence the transport in a large part of the plasma. As a result of these instabilities minor and major disruptions can occur. Double tearing modes can be stabilized by sheared (differential) rotation between the two rational surfaces.

#### H. Vertical Instability Of Elongated Plasmas

A circular shaped plasma is stable with respect to a axisymmetric vertical displacement as long as the field index defined by

$$n = -\frac{R}{B_v} \frac{dB_v}{dR} \quad (13)$$

is larger than zero. When the plasma cross section is elongated, the plasma column becomes unstable to a motion in the direction of elongation. If the plasma is surrounded by a conducting wall, this instability grows on the resistive time scale of the wall. Without conducting wall the growth rate, now determined by inertia, is larger. This instability can be controlled by active feedback stabilization using the poloidal field coil system. For example, the swiss tokamak TCV is designed for operation at large elongations (up to 3) and possesses an excellent feedback system which allows the control of growth rates of several  $1000\text{s}^{-1}$ . A passive stabilization by a conducting shell or conductors near the plasma is possible (similar to the external kink mode, RWM).

## V. RUNAWAY LIMIT

The toroidal electric field in a tokamak which is required to drive the ohmic current accelerates the electrons. The electric force is balanced by the drag due to collisions with electrons and ions. The slowing down time of the electrons decreases with increasing electron velocity. There is a critical velocity above which the electron is continuously accelerated. Even when the drift velocity of the bulk of the distribution function is small, electrons from the tail of the distribution can gain more and more energy, they *run away*. Runaway electrons can be accelerated to energies of several MeV

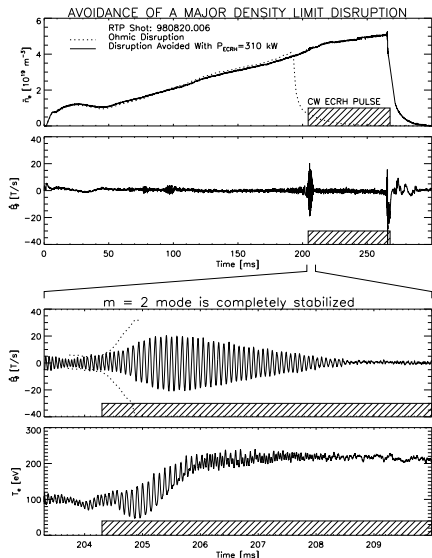


Figure 5: Avoidance of a disruption by ECR heating in RTP. (Figure supplied by F. Salzedas, IST Lisbon.)

and carry a considerably fraction of the plasma current. The generation of runaway electrons occurs when the plasma density is low and collisions are not very frequent. In the Hugill diagram (figure 1) the runaway region can be seen on the left side and gives a lower density limit. Runaway electrons do not only emerge on a long time scale during the discharge when the applied electric field is sufficiently high, but are as well created during disruptions [25]. These high energetic electron beams are a risk in large tokamaks because the interaction with the wall can evaporate wall material or even cause serious damage like melting of the wall.

## VI. DISRUPTIONS

In the previous sections we frequently mentioned the disruption of the tokamak discharge. In the disruption the energy from the plasma is released to the walls and the plasma current decays to zero. The evolution of a disruptions can be divided in several phases [6]. First there is an initiating event leading to an unstable situation. This is often caused by a modification of the plasma current distribution or a loss of plasma control. Precursor like mode oscillations appear next. The disruption itself has two phases: (i) the energy quench, where the plasma temperature collapses and the stored energy is released, and (ii) the current quench where the plasma current dies away.

The time constant for the exponential decay of the plasma current in the TEXTOR tokamak has been determined to be  $\tau_{I_p} = 14$  ms for standard conditions. Shorter time constants have been measured when the

impurity content in the plasma was high, resulting in a smaller conductivity, or when a part of the plasma current was transferred to the first wall and the time constant became as short as  $L/R = 3$  ms [26].

The sudden energy loss as well as the runaway electrons which are generated during a major disruption may damage the first wall. In addition large forces act on the vessel and supporting structures. These forces caused by *halo currents* which develop, when due to the displacement of the plasma column the plasma hits the wall and a fraction of the plasma current flows through wall elements where  $j \times B$  forces arise. Halo currents are produced, when the plasma position feedback is lost during a *vertical displacement event* (VDE) in elongated plasmas.

There are several experimental investigations on how a disruption can be prevented or ameliorated. One example is shown in figure 5. The density in this discharge is continuously increased until the density limit is encountered. Just prior to the disruption  $m = 2$  mode activity appears. Using strong electron cyclotron heating (ECH) the mode could be stabilized and the disruption prevented [27]. In the lower part of the figure one can see that after the start of ECH the mode amplitude drops to zero and the temperature rises. Finally, the plasma disrupts because the density has been increased even further.

Another possibility is the detection and stabilization of the disruption precursor mode [23]. Schemes for mitigation of disruptions use e.g. strong He gas puffs in order to avoid runaway production [28].

## VII. SUMMARY

In this article an overview on the constraints for tokamak operation has been given. The operational limits originate from various kinds of instabilities. Most serious are hard limitations like the  $q_a$ -limit or the radiation limit which lead to a disruption of the discharge and may do damage to the first wall or the supporting structures of the machine. Soft limitations like the onset of neoclassical tearing modes or the accumulation of impurities in the plasma result in a deterioration of the plasma confinement. The understanding of the operational boundaries is crucial for the optimization of tokamak performance in view of a large fusion experiment in the future. It has recently been shown that MHD activity like neoclassical tearing modes or  $m = 2, n = 1$  tearing modes as precursors to a disruption can be stabilized using various methods like electron cyclotron or lower hybrid current drive in order to control the plasma current profile. The early detection and the amelioration or prevention of a disruption using various means like localized ECR heating, creation

of sheared plasma rotation with neutral beam injection, or even the forced radiative collapse by injection of noble gases or so-called killer-pellets are presently under investigation. The Hugill diagram shows that the improvement of plasma parameters is closely linked to the development of wall coating techniques which improved the purity of the plasma.

## REFERENCES

1. F. Wagner et al., "Regime of improved confinement and high beta in neutral-beam-heated divertor discharges of the ASDEX tokamak", *Phys. Rev. Lett.*, **49**, 1408 (1982).
2. R. C. Wolf, "Internal transport barriers in tokamak plasmas", *Plasma Phys. Control. Fusion*, **45**, R1 (2003).
3. J. Rapp et al., "Scaling of Density Limits with Respect to Global and Edge Parameters in TEXTOR-94", *Proc. 26th Int. Conf. on Control. Fusion and Plasma Phys.*, Maastricht, **23J**, 665, European Physical Society, Geneva (1999).
4. J. Winter, "A Comparison of Tokamak Operation with Metallic Getters and Boronization", *J. Nucl. Mater.*, **176-177**, 14 (1990).
5. M. Greenwald, "Density Limits in Toroidal Plasmas", *Plasma Phys. Control. Fusion*, **44**, R27 (2002).
6. F. C. Schüller, "Disruptions in Tokamaks", *Plasma Phys. Control. Fusion*, **37**, A135 (1995).
7. B. Lipschultz, "Review of MARFE Phenomena in Tokamaks", *J. Nucl. Mater.*, **145-147**, 15 (1987).
8. J. Rapp et al., "Density Limits in TEXTOR-94 Auxiliary Heated Discharges", *Nucl. Fusion*, **39**, 765 (1999).
9. M. Greenwald et al., "A New Look at Density Limits in Tokamaks", *Nucl. Fusion*, **28**, 2199 (1988).
10. U. Samm et al., "Suppression of MARFEs by Plasma Position Feedback Control Based on Interferometric Measurements", *Proc. 18th Int. Conf. on Control. Fusion and Plasma Phys.*, Berlin, **15C**, part III, 137, European Physical Society, Geneva (1991).
11. J. Rapp et al., "Transport Studies of High-Z Elements in Neon Edge Radiation Cooled Discharges in TEXTOR-94", *Plasma Phys. Control. Fusion*, **39**, 1615 (1997).
12. M. Z. Tokar' et al., "The Influence of Impurities on Limiter Tokamak Plasmas and Relevant Mechanisms", *Plasma Phys. Control. Fusion*, **37**, A241 (1995).
13. H. R. Koslowski et al., "Characteristics of the  $q$  Profile for Different Confinement Conditions on TEXTOR-94", *Plasma Phys. Control. Fusion*, **39**, B325 (1997).
14. J. Wesson, "Hydromagnetic Stability of Tokamaks", *Nucl. Fusion*, **18**, 87 (1978).
15. F. Troyon et al., "MHD-Limits to Plasma Confinement", *Plasma Phys. Control. Fusion*, **26**, 209 (1984).
16. O. Sauter et al., "Beta Limits in Long-Pulse Tokamak Discharges", *Phys. Plasmas*, **4**, 1654 (1997).
17. H. R. Koslowski et al., "MHD Activity at the Beta Limit in RI-Mode Discharges on TEXTOR-94", *Nucl. Fusion*, **40**, 821 (2000).
18. H. R. Wilson, "Neoclassical tearing modes", *this proceedings*.
19. H. Zohm et al., "Experiments on Neoclassical Tearing Mode Stabilization by ECCD in ASDEX-Upgrade", *Nucl. Fusion*, **39**, 577 (1999).
20. C. D. Warrick et al., "Complete Stabilization of Neoclassical Tearing Modes with Lower Hybrid Current Drive on COMPASS-D", *Phys. Rev. Lett.*, **85**, 574 (2000).
21. Q. Yu et al., "Stabilization of Neoclassical Tearing Modes by an Externally Applied Static Helical Field", *Phys. Rev. Lett.*, **85**, 2949 (2000).
22. S. Günter et al., "High-confinement regime at high  $\beta_N$  values due to a changed behavior of the neoclassical tearing modes", *Phys. Rev. Lett.*, **87**, 275001 (2001).
23. A. Krämer-Flecken et al., "Heterodyne ECE Diagnostic in the Mode Detection and Disruption Avoidance at TEXTOR", *Nucl. Fusion*, in press (2003).
24. M. Okabayashi et al., "Stabilization of the Resistive Wall Mode in DIII-D by Plasma Rotation and Magnetic Feedback", *Plasma Phys. Control. Fusion*, **44**, B339 (2002).
25. R. Jaspers et al., "Disruption Generated Runaway Electrons in TEXTOR and ITER", *Nucl. Fusion*, **36**, 367 (1996).
26. G. Waidmann et al., "Density Limits and Evolution of Disruptions in Ohmic TEXTOR Plasmas", *Nucl. Fusion*, **32**, 645 (1992).
27. F. Salzedas et al., "Stabilization, with ECRH, of an  $m/n = 2/1$  Tearing Mode Preceding a Radiative Density Limit Disruption", *Proc. 26th Int. Conf. on Control. Fusion and Plasma Phys.*, Maastricht, vol 23J, p 625, European Physical Society, Geneva (1999).
28. K. H. Finken et al., "Mitigation of Disruptions by Fast Helium Gas Puffs", *Nucl. Fusion*, **41**, 1651 (2001).